THE DESIGN OF MULTI-DIMENSIONAL COMPLEX-VALUED FIR DIGITAL FILTERS BY PROJECTIONS ONTO CONVEX SETS

W. A. Mousa, D. C. McLernon, and S. Boussakta

School of Electronic & Electrical Engineering
The University of Leeds
Leeds LS2 9JT, United Kingdom
WMousa@slb.com, D.C.Mclernon@leeds.ac.uk, S.Boussakta@leeds.ac.uk

ABSTRACT

We propose the design of multi-dimensional (m-D) complex-valued FIR digital filters using the thoery of Projection onto Convex Sets (POCS). The proposed design algorithm is a generalization of the one-dimensional (1-D) real-valued FIR filter design cases reported in [1, 2] to m-D complex-valued FIR filters. Simulation results show that the resulting frequency responses possess an approximate equiripple nature. Also, they illustrate superior designs using POCS when compared with the complex Remez filter design method previously reported in [3].

1. INTRODUCTION

Most of the existing FIR design techniques assume zero/linear phase FIR filters which result in filters having real-valued FIR coefficients. However, in certain applications, like the case of seismic migration filters, both the magnitude and the phase responses need to be of even symmetry and the phase is non-linear, and this results in FIR filter coefficients being complex-valued [4, 3]. Also, a low delay single passband filter is another example of the need for complex-valued FIR filters [5].

Some researchers approach the problem of designing filters with complex coefficients by expressing the desired phase and magnitude responses as complex Cartesian components and operate on the real and imaginary components independently. Then, the final filter coefficients are formed from the resultant real and imaginary coefficients [6]. Moreover, Chen-Parks [7] approximate the complex-valued response by a real-valued function and the resulting errors in magnitude and group delay are made approximately equiripple. Their method, however, requires large computer memory and the design-time increases exponentially with increasing time and frequency grid-density [7, 2]. In another development, Karam and McClellan [4, 3], have extended the Parks-McClellan (Remez exchange) algorithm [8, 6] for complex-valued FIR filter design. The simulation results indicate that this algorithm is efficient in terms of memory and speed convergence. However, as in the case of the Remez exchange algorithm, it is not easy to extend the algorithm to m-D FIR filter design. In addition, more constraints cannot be incorporated into the design specifications.

Recently, a novel iterative FIR filter design algorithm was introduced (based on one forward and one inverse Fast Fourier Transform (FFT)) to design zero-phase FIR filters [1]. The algorithm alternately satisfies the frequency domain constraints on the magnitude response bounds as well as time domain constraints on the impulse response support [1]. The main advantages of this method are based on its implementation simplicity and versatility. This algorithm is known as *Projection onto Convex Sets (POCS)*. This idea was similarly used in [9] for the design of arbitrary complex frequency response. However, both algorithms were derived heuristically without explicitly defining the constraint sets properly and deriving their associated projections. In addition, the heuristic nature of such approaches does not obviously lend itself to the design of filters with other constraints. Recently in [2], the proper mathematical way to derive the design algorithm of real-valued linear-phase FIR 1-D filters using POCS was shown. The POCS theory leads to a feasible solution which satisfies all predefined constraint sets. The constraint sets are formulated as sets that are closed and convex within a suitable Hilbert space [2]. In [2] the Hilbert space was the M-dimensional Euclidean space. Moreover, unlike many FIR filter design techniques, the POCS approach for designing FIR filters can easily be directly extended to the design of m-D filters. Furthermore, for the case of designing FIR digital filters, the POCS will require only two FFT computations per iteration [1].

Therefore, a novel algorithm for the design of m-D complex-valued FIR digital filters using the method of Projections onto Convex Sets (POCS) is derived in this paper. This is achieved by extending the work carried out for designing 1-D real-valued FIR digital filters using POCS (as reported in [2]) to the more general class of m-D complex-valued FIR filters which are important in many applications as stated earlier. This paper starts with a brief background about POCS in section 2. Then section 3 deals with the derivation of the design algorithm for complex-valued filters where the m-D complex-valued FIR filter design algorithm using POCS is stated. Simulation results are given in section 4 and finally in section 5 presents some conclusions.

2. OVERVIEW OF PROJECTIONS ONTO CONVEX SETS

The approach of POCS has recently been used in a number of applications [10]. However, for the understanding of this paper, it is necessary to basically re-state the theory of POCS. To begin with, let all the filters of interest be elements of a Hilbert space $\mathbf{H}$ and consider a closed convex set C which is a subset of $\mathbf{H}$. Then, for any vector $\mathbf{h} \in \mathbf{H}$, the projection $P_C\mathbf{h}$ of $\mathbf{h}$ onto C (where P_C is an operator) is the nearest neighbor element in C to $\mathbf{h}$ (i.e., $\mathbf{y}$) and is determined by

$$\|\mathbf{h} - P_C\mathbf{h}\| = \min_{\mathbf{y}\in C}\|\mathbf{h} - \mathbf{y}\| \tag{1}$$

where $\|\cdot\|$ is the Euclidean norm. The operator P_C is a nonlinear projection operator that maps any vector $\mathbf{h} \in \mathbf{H}$ to a vector that belongs to C. Now the basic idea of POCS is as follows. Every known property of the unknown $\mathbf{h} \in \mathbf{H}$ will restrict $\mathbf{h}$ to lie in a closed convex set, say $C_i \in \mathbf{H}$. Assume that $C_1, C_2, \cdots, C_l$ denote l (for l known properties) closed convex sets in a Hilbert space $\mathbf{H}$, and C_o denotes their

intersection set given by

$$C_o = \bigcap_{i=1}^{l} C_i. \tag{2}$$

The set C_o, which is considered as the solution set, will contain elements that satisfy all the constraint sets and will therefore represent feasible solutions. For each $i = 1, 2, \cdots, l$, let P_{C_i} denote the projection operator onto the set C_i. Then, the Fundamental Theorem of POCS is given as follows [10]:

Theorem 1 *Assume that C_o is non-empty. Then for every $\mathbf{h} \in \mathbf{H}$ and $i = 1, 2, \cdots, l$, the sequence $\{P_{C_i}\mathbf{h}\}$ converges weakly to a point of C_o.*

In other words, theorem 1 states that the vector iterates $\{\mathbf{h}_k\}$ generated by

$$\mathbf{h}_{k+1} = P_{C_l} P_{C_{l-1}} \cdots P_{C_1} \mathbf{h}_k \tag{3}$$

with an arbitrary starting point $\mathbf{h}_0$, will converge weakly to a point of C_o, and since our Hilbert space is of finite dimension, the algorithm will strongly converge to a point within C_o [11, 10].

3. COMPLEX-VALUED FIR FILTER DESIGN USING POCS

In order to design m-D complex-valued FIR digital filters using POCS, we need to derive the design algorithm for the 1-D complex case. Hence, let us design N-length 1-D complex-valued FIR digital filters using POCS, where the required filter properties are put into constraint sets that are closed convex sets belonging to the set of M-dimensional complex vectors, i.e., $\mathbf{H} = \mathbb{C}^M$ where $M \gg N$. In this case, the properties are from the time domain and also frequency domain. So we want to design an N-length FIR filter $h[n]$ which is complex-valued. The magnitude spectrum of the discrete time Fourier transform (DTFT) of $h[n]$ must be upper and lower bounded by $1+\delta_p$ and $1-\delta_p$, respectively in the passband. In addition, the stopband magnitude spectrum must be bounded by δ_s. Finally, we want the phase spectrum to be as close as possible to a predefined phase, say $\phi(\omega)$. If these constraint sets are closed convex sets, and happen to intersect, then we can guarantee strong convergence of the algorithm since our space is of finite dimension. So the following sections represent the constraint sets. Note that we can show that they are closed convex sets and also that we can derive their associated projection operators.

3.1 The constraint set C_1

Let $C_1 = \{\mathbf{h} \in \mathbb{C}^M : h[n] = 0 \text{ for } n \notin S\}$ where S is the set of points on which the filter coefficients of length N are not equal to zero. That is, C_1 is the set of all complex-valued vectors of length M with at most N non-zero filter coefficients. The projection of an arbitrary vector $\mathbf{x} \in \mathbb{C}^M$, where $\mathbf{x} \notin C_1$, onto C_1, i.e., P_{C_1}, can be given by the following relationship:

$$P_{C_1}\mathbf{x} = \begin{cases} x[n], \text{ if } n \in S \\ 0, \text{ if } n \notin S. \end{cases} \tag{4}$$

3.2 The constraint set C_2

$C_2 = \{\mathbf{h} \in \mathbb{C}^M \text{ with } h[n] \leftrightarrow H(e^{j\omega}) : \angle H(e^{j\omega}) = \phi(\omega)\}$. That is, C_2 is the set of all sequences which are complex-valued and whose phase response is constrained to be equal to a predefined phase response $\phi(\omega)$. The projection of $\mathbf{x} \in \mathbb{C}^M$ and $\mathbf{x} \notin C_2$ onto C_2 can be given by the following equation:

$$P_{C_2}\mathbf{x} \leftrightarrow \begin{cases} |X(e^{j\omega})| \cos(\theta_x - \phi(\omega)) \exp(j\phi(\omega)), \text{ if } A_{C_2} \\ -|X(e^{j\omega})| \cos(\theta_x - \phi(\omega)) \exp(j\phi(\omega)), \text{ if } B_{C_2} \end{cases} \tag{5}$$

where $A_{C_2} \Rightarrow \cos(\theta_x - \phi(\omega)) \geq 0$, and $B_{C_2} \Rightarrow \cos(\theta_x - \phi(\omega)) < 0$.

3.3 The constraint set C_3

Define C_3 as the set of complex-valued sequences whose DTFT magnitude spectrum is lower bounded by $1-\delta_p$ in the passband, i.e., $C_3 = \{\mathbf{h} \in \mathbb{C}^M \text{ with } h[n] \leftrightarrow H(e^{j\omega}) : |H(e^{j\omega})| \geq 1-\delta_p \text{ for } \omega \in \Omega_p\}$ where Ω_p is the passband interval which is equal to $[-\omega_p, \omega_p]$, ω_p is the cut-off frequency, and δ_p is the maximum passband allowable tolerance. The projection P_{C_3} onto C_3 of an arbitrary vector $\mathbf{x} \in \mathbb{C}^M$, where $\mathbf{x} \notin C_3$, can be written as

$$P_{C_3}\mathbf{x} \leftrightarrow \begin{cases} X(e^{j\omega}), \text{ if } |X(e^{j\omega})| > (1-\delta_p) \text{ for } \omega \in \Omega_p \\ (1-\delta_p)\frac{X(e^{j\omega})}{|X(e^{j\omega})|}, \text{ if } |X(e^{j\omega})| \leq (1-\delta_p) \text{ for } \omega \in \Omega_p \\ X(e^{j\omega}), \text{ otherwise.} \end{cases} \tag{6}$$

3.4 The constraint set C_4

Let $C_4 = \{\mathbf{h} \in \mathbb{C}^M \text{ with } h[n] \leftrightarrow H(e^{j\omega}) : |H(e^{j\omega})| \leq 1+\delta_p \text{ for } \omega \in \Omega_p\}$. So we can say that C_4 is the set of complex-valued sequences whose DTFT magnitude should not exceed the limit $1+\delta_p$ in the passband. Also, it can be shown that the projection of an arbitrary vector $\mathbf{x} \in \mathbb{C}^M$, where $\mathbf{x} \notin C_4$, is given by

$$P_{C_4}\mathbf{x} \leftrightarrow \begin{cases} X(e^{j\omega}), \text{ if } |X(e^{j\omega})| < (1+\delta_p) \text{ for } \omega \in \Omega_p \\ -(1+\delta_p)\frac{X(e^{j\omega})}{|X(e^{j\omega})|}, \text{ if } |X(e^{j\omega})| \geq (1+\delta_p) \text{ for } \omega \in \Omega_p \\ X(e^{j\omega}), \text{ otherwise.} \end{cases} \tag{7}$$

3.5 The constraint set C_5

Finally, let C_5 be the set of all sequences which are complex-valued and whose DTFT magnitude is bounded by δ_s in the stopband Ω_s where $\Omega_s = [-\pi, -\omega_s) \cap (\omega_s, \pi]$, ω_s is the stopband cut-off frequency and δ_s is the maximum allowable stopband tolerance. So $C_5 = \{\mathbf{h} \in \mathbb{C}^M \text{ with } h[n] \leftrightarrow H(e^{j\omega}) : |H(e^{j\omega})| \leq \delta_s \text{ for } \omega \in \Omega_s\}$. Finally, the projection of an arbitrary vector $\mathbf{x} \in \mathbb{C}^M$, where $\mathbf{x} \notin C_5$, can be shown to be

$$P_{C_5}\mathbf{x} \leftrightarrow \begin{cases} X(e^{j\omega}), \text{ if } |X(e^{j\omega})| < \delta_s \text{ for } \omega \in \Omega_s \\ -\delta_s\frac{X(e^{j\omega})}{|X(e^{j\omega})|}, \text{ if } |X(e^{j\omega})| \geq \delta_s \text{ for } \omega \in \Omega_s \\ X(e^{j\omega}), \text{ otherwise.} \end{cases} \tag{8}$$

3.6 The POCS design algorithm for m-D complex-valued FIR filters

Following from (3), the POCS algorithm for designing 1-D complex-valued FIR digital filters is given by

$$\mathbf{h}_{k+1} = P_{C_1} P_{C_2} P_{C_3} P_{C_4} P_{C_5} \mathbf{h}_k \tag{9}$$

where P_{C_1}, P_{C_2}, P_{C_3}, P_{C_4}, and P_{C_5} are given in (4), (5), (6), (7), and (8), respectively, and $\mathbf{h}_0$ is an arbitrary complex-valued vector of dimension M. Now, as mentioned earlier, one of the main advantages of using POCS to design FIR digital filters is the simplicity of extending the 1-D design algorithm to multi-dimensions. So we are interested in extending the 1-D complex-valued FIR filter design algorithm to m-D as shown below.

1. Project $\mathbf{h}_k$ onto C_5, that is

$$\mathbf{g}_{1,k} = P_{C_5}\mathbf{h}_k \leftrightarrow \begin{cases} H_k(e^{j\mathbf{\Omega}}), \text{ if } A_{C_5} \\ -\delta_s \frac{H_k(e^{j\mathbf{\Omega}})}{|H_k(e^{j\mathbf{\Omega}})|}, \text{ if } B_{C_5} \\ H_k(e^{j\mathbf{\Omega}}), \text{ otherwise} \end{cases} \tag{10}$$

where $A_{C_5} \Rightarrow |H_k(e^{j\mathbf{\Omega}})| < \delta_s$ for $\mathbf{\Omega} \in \mathbf{\Omega}_s$, and $B_{C_5} \Rightarrow |H_k(e^{j\mathbf{\Omega}})| \geq \delta_s$ for $\mathbf{\Omega} \in \mathbf{\Omega}_s$.

2. Project $\mathbf{g}_{1,k}$ onto C_4 using

$$\mathbf{g}_{2,k} = P_{C_4}\mathbf{g}_{1,k} \leftrightarrow \begin{cases} G_{1,k}(e^{j\mathbf{\Omega}}), \text{ if } A_{C_4} \\ -(1+\delta_p) \frac{G_{1,k}(e^{j\mathbf{\Omega}})}{|G_{1,k}(e^{j\mathbf{\Omega}})|}, \text{ if } B_{C_4} \\ G_{1,k}(e^{j\mathbf{\Omega}}), \text{ otherwise} \end{cases} \tag{11}$$

where $A_{C_4} \Rightarrow |G_{1,k}(e^{j\mathbf{\Omega}})| < (1+\delta_p)$ for $\mathbf{\Omega} \in \mathbf{\Omega}_p$, and $B_{C_4} \Rightarrow |G_{1,k}(e^{j\mathbf{\Omega}})| \geq (1+\delta_p)$ for $\mathbf{\Omega} \in \mathbf{\Omega}_p$.

3. Project $\mathbf{g}_{2,k}$ onto C_3 using

$$\mathbf{g}_{3,k} = P_{C_3}\mathbf{g}_{2,k} \leftrightarrow \begin{cases} G_{2,k}(e^{j\mathbf{\Omega}}), \text{ if } A_{C_3} \\ (1-\delta_p) \frac{G_{2,k}(e^{j\mathbf{\Omega}})}{|G_{2,k}(e^{j\mathbf{\Omega}})|}, \text{ if } B_{C_3} \\ G_{2,k}(e^{j\mathbf{\Omega}}), \text{ otherwise} \end{cases} \tag{12}$$

where $A_{C_3} \Rightarrow |G_{2,k}(e^{j\mathbf{\Omega}})| > (1-\delta_p)$ for $\mathbf{\Omega} \in \mathbf{\Omega}_p$, and $B_{C_3} \Rightarrow |G_{2,k}(e^{j\mathbf{\Omega}})| \leq (1-\delta_p)$ for $\mathbf{\Omega} \in \mathbf{\Omega}_p$.

4. Project $\mathbf{g}_{3,k}$ onto C_2 using

$$\mathbf{g}_{4,k} = P_{C_2}\mathbf{g}_{3,k} \leftrightarrow \begin{cases} |G_{3,k}(e^{j\mathbf{\Omega}})|\mathbf{\Gamma} \text{ if } A_{C_2} \\ -|G_{3,k}(e^{j\mathbf{\Omega}})|\mathbf{\Lambda} \text{ if } B_{C_2} \end{cases} \tag{13}$$

where $\mathbf{\Gamma} = \cos\left(\theta_{G_{3,k}} - \phi(\mathbf{\Omega})\right)\exp(j\phi(\mathbf{\Omega}))$, $A_{C_2} \Rightarrow \cos\left(\theta_{G_{3,k}} - \phi(\mathbf{\Omega})\right) \geq 0$, $\mathbf{\Lambda} = \cos\left(\theta_{G_{3,k}} - \phi(\mathbf{\Omega})\right)$ $\exp(j\phi(\mathbf{\Omega}))$, and $B_{C_2} \Rightarrow \cos\left(\theta_{G_{3,k}} - \phi(\mathbf{\Omega})\right) < 0$.

5. Finally, project $\mathbf{g}_{4,k}$ onto C_1 by

$$\mathbf{h}_{k+1} = P_{C_1}\mathbf{g}_{4,k} = \begin{cases} \mathbf{g}_{4,k}[\mathbf{n}], \text{ for } \mathbf{n} \in \mathbf{S} \\ 0, \text{ otherwise} \end{cases} \tag{14}$$

where $\mathbf{\Omega} = (\omega_1, \omega_2, \cdots, \omega_m)$ and $\boldsymbol{n} = (n_1, n_2, \cdots, n_m)$, $\mathbf{S}$ is the m-D finite extent support, $\mathbf{\Omega}_p$ is the m-D passband region, and $\mathbf{\Omega}_s$ is the m-D stopband region. In this paper, the same stopping criterion reported in [2] is used. That is, if the distance error is less than or equal to a predefined threshold ϵ, i.e., if $\|\mathbf{h}_{k+1} - \mathbf{h}_k\| \leq \epsilon$, then we will stop the algorithm. Otherwise, we will repeat steps 1-5.

4. SIMULATION RESULTS

Recall that M is the dimension of the Hilbert space, N is the filter length, δ_p and δ_s are respectively the maximum allowable passband and stopband tolerances, and ϵ is the algorithm stopping threshold. Note that the simulations are preformed in MATLAB which is installed on a Pentium 4 machine with a speed of 2.6 GHz and with a RAM of 1GB. Finally, the designed filters are displayed with respect to their normalized angular frequencies.

4.1 Low Delay Non-Symmetric Passband Filters

Low delay non-symmetric passband FIR filters are used in many areas of application such as communications [5]. Here, we illustrate the design of two low delay single passband FIR filters: 1-D and 2-D filters designed using POCS.

4.1.1 A 1-D Low Delay Non-Symmetric Passband Filter

An example of a desired low delay filter can be given by:

$$H_d(e^{j\omega}) = \begin{cases} e^{-j12\omega}, & \text{if } -0.1\pi \leq \omega \leq 0.3\pi \\ 0, & \text{if } -\pi \leq \omega \leq -0.2\pi \ \& \ 0.4\pi \leq \omega \leq \pi \end{cases} \tag{15}$$

where $\delta_p = 0.00025$, $\delta_s = 0.025$, $N = 31$, $M = 310$, and with a stopping threshold equal to $\epsilon = 10^{-5}$. In Fig. 1 (a), the designed magnitude response of the filter shows an approximate equiripple response with a maximum stopband magnitude of -29 dB. The group delay is shown in Fig. 1 (b) where it corresponds to almost linear-phase characteristics in the passband with a mean absolute deviation (we take the mean of the absolute value within the passband group delay difference between the ideal and designed filters) from the desired group delay of 4.3993×10^{-2}. As can be seen clearly from Fig. 1 (c), the design required 129 iterations to uniformly converge with $\epsilon = 10^{-5}$ and it took 0.54 secs. The same filter was designed using the complex Remez exchange algorithm reported in [3] with a passband weight of 10. The algorithm, which is written as a MATLAB built-in function, took 8.08 secs on the same machine. The magnitude spectrum of this filter is also shown in Fig. 1 (a) where its stopband magnitude is approximately equal to -23 dB while its group delay mean absolute deviation from the desired group delay is equal to 5.28 (see Fig. 1 (b)). The POCS designed filter in this case resulted in a better magnitude response as well as a better group delay response when compared with that obtained using the complex Remez method. Also, in this case, the POCS design algorithm required less design running time (it saved 93.81% of the design running time) when compared to the complex Remez low delay single passband designed filter.

4.1.2 A 2-D Low Delay Shifted Circularly Symmetric Filter

We want to design a 2-D complex-valued FIR low delay filter based on a passband and stopband circular specifications. The circular region is centered on $(-0.1\pi, 0.1\pi)$ with a passband radius of 0.3π and a stopband radius of 0.5π. The filter parameters are as follows: $\delta_p = \delta_s = 25 \times 10^{-3}$, for a 19×19 filter, $M = 190 \times 190$, and with a delay of 9 samples. The design took 372 iterations to converge with an error threshold of $\epsilon = 5 \times 10^{-5}$. Fig. 2 shows the circularly symmetrical magnitude response of the designed filter, where it satisfies the aforementioned design specifications.

5. CONCLUSION

This paper has extended the design of 1-D real-valued FIR digital filters using the theory of *Projections onto Convex Sets* (POCS) to include m-D complex-valued FIR digital filters. So this newly derived POCS algorithm for m-D complex-valued FIR filters is more general and can also accommodate m-D real-valued filters. The resultant filters possess an approximate equiripple behavior. The simulation results have illustrated a superior filter design when using POCS, when compared with the complex Remez filter design method reported previously in [3]. The only disadvantage of the POCS algorithm for FIR filter design (in the opinion of some filter designers), and depending upon the filter parameters and stopping threshold value, is the large number of iterations required to achieve convergence. One can overcome this problem by speeding up the convergence of the POCS design algorithm for FIR filter design by using the relaxed version of POCS, which is known as: *Relaxed Projections onto Convex Sets* [10].

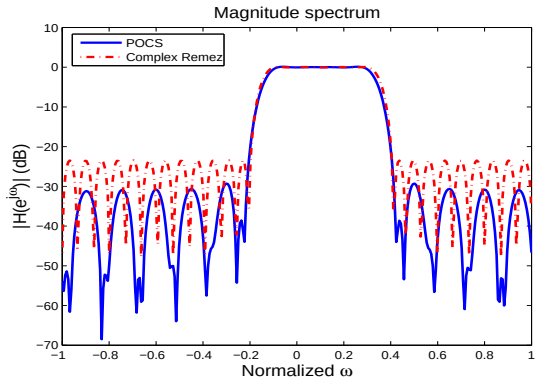

(a)

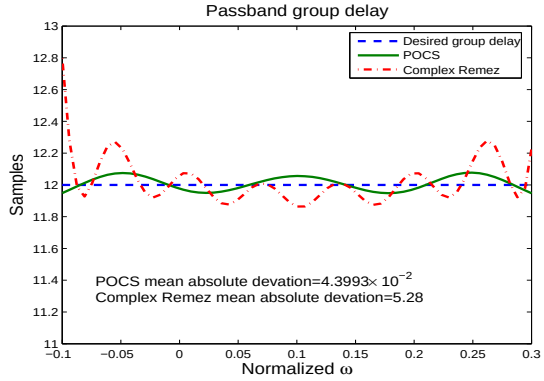

(b)

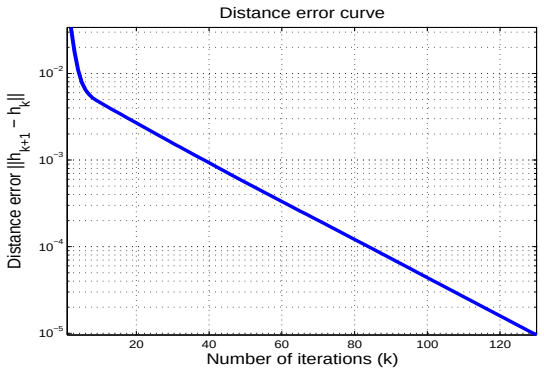

(c)

Figure 1: A 1-D complex-valued low delay FIR low-pass filter with $N = 31$, $M = 310$, $\omega_{p_1} = -0.1\pi$, $\omega_{p_2} = 0.3\pi$, $\omega_{s_1} = -0.2\pi$, $\omega_{s_2} = 0.4\pi$ $\delta_p = 0.00025$, $\delta_s = 0.025$, and $\epsilon = 10^{-5}$: (a) magnitude response in dB (POCS: solid line and Complex Remez: dash-dot line), (b) passband group delay (POCS: solid line, Complex Remez: dash-dot line and the Desired Group Delay: dash line), and (c) convergence of the 1-D complex-valued low delay FIR low-pass filter design using POCS distance error curve.

6. ACKNOWLEDGMENT

The authors would like to acknowledge Schlumberger Dhahran Carbonate Research, Dhahran, Saudi Arabia, for sponsoring this work.

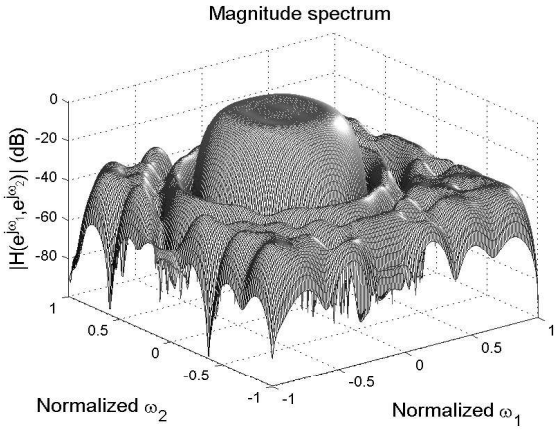

Figure 2: The magnitude response in dB of a 2-D complex-valued low 9 sample delay (shifted) circularly symmetric FIR filter designed using POCS with $N \times N = 19 \times 19$, $M \times M = 190 \times 190$, centered at $(-0.1\pi, 0.1\pi)$ with passband radius of 0.3π, stopband radius of 0.5π, $\delta_p = \delta_s = 25 \times 10^{-3}$, and $\epsilon = 5 \times 10^{-5}$.

REFERENCES

[1] A. E. Çetin, O. N. Gerek, and Y. Yardimci, "Equiripple FIR filter design by the FFT algorithm," *Signal Processing Magazine, IEEE*, vol. Vol.14, pp. 60–64, Mar 1997.

[2] K. C. Haddad, H. Stark, and N. P. Galatsanos, "Constrained FIR filter design by the method of vector space projections," *IEEE Trans. on Circuits and Systems*, vol. 47, no. 8, pp. 714 – 725, August 2000.

[3] L. J. Karam and J. H. McClellan, "Chebyshev digital FIR filter design," *Signal Processing*, vol. 76, pp. 17 – 36, 1999.

[4] L. Karam and J. McClellan, "Complex Chebyshev approximation for FIR filter design," *IEEE Trans. on Circuits and Systems*, vol. 42, no. 3, pp. 207 – 216, March 1995.

[5] S. C. Chan and K. M. Tsui, "On the design of real and complex FIR filters with flatness and peak error constraints using semidefinite programming," International Symposium on Circuits and Systems (ISCAS'04), 2004, vol. 3, pp. III: 125–128.

[6] V. K. Madisetti and D. B. Williams, Eds., *The Digital Signal Processing Handbook*, CRC Press and IEEE Press, 1998.

[7] X. Chen and T. Parks, "Design of FIR filters in the complex domain," *IEEE Trans. on Acoustics, Speech, and Signal Processing*, vol. 35, no. 2, pp. 144 – 153, Feb. 1987.

[8] L. B. Jackson, *Digital Filters and Signal Processing*, Kluwer Academic Publisher, 3rd edition, 1996.

[9] E. Hermanowicz and M. Blok, "Iterative technique for approximate minimax design of complex digital fir filters," *7th IEEE International conference on Electronics, Circuits and Systems*, vol. 1, pp. 83–86, 2000.

[10] H. Stark and Y. Yang, *Vector Space Projections: a numerical approach to Signal and Image processing, Neural nets, and Optics*, John Wiley and Sons Publisher, 1st edition, 1998.

[11] E. Kreyszig, *Introductory Functional Analysis with Applications*, John Wiley and Sons, 1978.